

## Research Article

# Research on the Properties of Low Temperature and Anti-UV of Asphalt with Nano-ZnO/Nano-TiO<sub>2</sub>/Copolymer SBS Composite Modified in High-Altitude Areas

Xiangbing Xie <sup>1</sup>, Tao Hui,<sup>2</sup> Yaofei Luo,<sup>1</sup> Han Li,<sup>1</sup> Guanghui Li <sup>1</sup> and Zhenyu Wang<sup>1</sup>

<sup>1</sup>School of Civil Engineering and Architecture, Zhengzhou University of Aeronautics, Zhengzhou, Henan 450046, China

<sup>2</sup>Zhengzhou Communications Planning Survey & Design Institute, Zhengzhou, China

Correspondence should be addressed to Guanghui Li; [lgh@zua.edu.cn](mailto:lgh@zua.edu.cn)

Received 18 December 2019; Revised 19 February 2020; Accepted 3 March 2020; Published 30 April 2020

Academic Editor: Michael Aizenshtein

Copyright © 2020 Xiangbing Xie et al. This is an open access article distributed under the Creative Commons Attribution License, which permits unrestricted use, distribution, and reproduction in any medium, provided the original work is properly cited.

Strong ultraviolet light and low-temperature are the typical environmental characteristics in high-altitude areas. The performance of SBS-modified asphalt in the above environmental characteristics needs further study. To improve the resistance ultraviolet (UV) ageing and low-temperature performance of copolymer- (SBS-) modified asphalt, an SBS-modified asphalt containing nano-ZnO and nano-TiO<sub>2</sub> is proposed. In this paper, nano-ZnO, nano-TiO<sub>2</sub>, and SBS were used as modifiers with the silane coupling agent (KH-560) as the nanomaterial surface modification. The orthogonal test table was used to analyse the effects of the three modifiers on the physical properties of modified asphalt at different dosages. On this basis, the physical properties, low-temperature properties, and ageing indices (carbonyl index and sulfoxide index) were studied for base asphalt, SBS-modified asphalt, nano-ZnO/SBS-modified asphalt, and nano-ZnO/nano-TiO<sub>2</sub>/SBS composite-modified asphalt before and after photoaging. The content changes of characteristic elements (Zn and Ti) in the nano-ZnO/nano-TiO<sub>2</sub>/SBS composite-modified asphalt before and after ageing were studied by scanning electron microscopy with energy dispersive spectroscopy (SEM/EDS), and the UV ageing mechanism was revealed. The results indicate that two nanoparticles show the best compatibility with asphalt after surface modification and can improve the binding ability between SBS and base asphalt. The orthogonal test analysis shows that nano-ZnO has a highly significant effect on the low- and high-temperature performance of the nano-ZnO/nano-TiO<sub>2</sub>/SBS composite-modified asphalt, and nano-TiO<sub>2</sub> has a significant effect on the high-temperature performance. Three optimal composite-modified systems for base asphalt including 4% nano-ZnO/1.5% nano-TiO<sub>2</sub>/3.2% SBS were proposed and had the best antiaging ability. Compared with the sulfoxide index, the carbonyl index changed most obviously before and after ageing. Additionally, the results reveal that nano-TiO<sub>2</sub> has a good absorption effect at a wavelength of 365 nm (ultraviolet light), while nano-ZnO is liable to photolysis, and its activity decreases at this wavelength.

## 1. Introduction

In highway pavement engineering at high altitudes, the styrene-butadiene-styrene (SBS) block copolymer-modified asphalt is mostly used as a binder in the surface layer. Due to the long-term exposure to intense ultraviolet light, the ultraviolet (UV) ageing of SBS-modified asphalt tends to be photooxidation ageing [1–3]. Compared with the UV ageing of the base asphalt, the SBS-modified asphalt is affected by the base asphalt and SBS modifier; for example, the content of asphaltene depends on the synergistic effect between them [4–6]. During the ageing process, butadiene

in SBS copolymers is degraded, the base asphalt is oxidized, and the ageing indices (sulfoxide index and carbonyl index) gradually increase. SBS modifier degradation could slow down the aging reaction of matrix asphalt, and the matrix asphalt could also play a role in the protection of the SBS modifier. Their interaction can effectively delay the ageing rate of SBS-modified asphalt [5, 7]. However, due to the considerable difference in physical properties between SBS copolymers and base asphalt [7, 8], the compatibility and dispersion of SBS-modified asphalt are generally poor, which affects the ageing resistance of the modified asphalt.

Currently, nanomaterials have been widely used due to their unique properties in improving the properties of asphalt. For example, Li et al. reported the effect of nano-ZnO with modified surface on the physical and anti-UV ageing properties of base asphalt and found that the surface-modified nano-ZnO obviously increased the softening point, viscosity, and ageing resistance of binder, as well as improving the ductility of bitumen [9]. Zhu investigated the effect of nano-ZnO on pavement performance of SK-70 base asphalt through differential scanning calorimetry (DSC), dynamic shear rheometer (DSR), and Brinell viscometer, and the results showed that nano-ZnO could improve significantly the low-temperature ductility, high-temperature rutting resistance, and ageing resistance of asphalt [10]. Another study by Liu et al. showed that the dispersion stability of nano-ZnO in bitumen was improved by surface modifiers and could improve the anti-UV properties of asphalt [11]. Fang et al. concluded that the low-temperature anticracking properties had been improved significantly by adding nano-ZnO particles into asphalt [12]. Zheng et al. study showed that addition of nano-TiO<sub>2</sub> could improve UV-aging resistance of asphalt, with no obvious influence on low-temperature rheology [2]. Xu et al. indicated that nano-ZnO as an additive could improve the softening point, ductility (5°C), rheological properties, and fatigue performance of base asphalt [13]. Wang et al. conducted research on the effect of inorganic nanoparticles (nano-SiO<sub>2</sub>, nano-TiO<sub>2</sub>, and nano-ZnO) combined with organic expanded vermiculite (OVEMT) on asphalt binder and showed that other multiscale nanocomposites made the continuous PG grading temperature lower than base asphalt on the low-temperature property, except for 1% OVEMT plus 3% nano-SiO<sub>2</sub> [14]. Kleizienė et al. reported that nanoparticles (nano-SiO<sub>2</sub>, nano-TiO<sub>2</sub>, and nano-ZnO) as modification additive have the potential to enhance the complex shear modulus and reduce the phase angle of base asphalt, and the excessive amount of nanomaterials might result in the lower asphalt binder resistant to fatigue [15]. Saltan et al. indicated that the addition of zinc oxide nanoparticle (ZnONP) was able to improve permanent deformation and the resistance to thermal cracking compared to the neat bitumen [16]. Nazari et al. illustrated that the addition of nano-TiO<sub>2</sub> nanoparticles improved the aging resistance of asphalt binder [17]. Zhang and Zhang suggested that the ductility at 10°C of modified bitumen with nano-ZnO surface modification increased about 12 cm and the anti-UV aging ability enhanced significantly compared to those of base asphalt [18]. Hamedi et al. showed that the nano-ZnO was highly improved on the adhesion of asphalt-aggregate in wet conditions [19]. Moreover, many researchers studied the effect of the content or types of nanomaterial on the performance of asphalt. Salton et al. evaluated the effect of the content of zinc oxide nanoparticles (nano-ZnO) on permanent deformation of modified asphalt; the results showed that 5% modification had the best performance [16]. The study of Zhu et al. illustrated that 3% nano-ZnO and 1% organic expanded vermiculite (OEVMT) could improve the shear deformation resistance and elastic behavior of SBR modified asphalt [20]. Azarhoosh et al. analysed hot mix

(HMA) asphalt containing 1%, 3%, 5%, and 7% of nano-ZnO mixed with bitumen 85/100. The results showed that fatigue life of mixtures containing nano-ZnO was higher than those of the control mixtures due to improved cohesion energy and higher resistance to fatigue cracking in asphalt [21]. In order to examine the role of nanomaterial in the ageing process of asphalt, Zhang and Zhang further found that the improved anti-UV aging performance could be attributed to the shielding function of inorganic nanoparticles to UV radiation [5, 18, 22]. In addition, many researchers extensively studied the properties of nano-TiO<sub>2</sub> modified asphalt. For example, Azarhoosh et al. found that nano-TiO<sub>2</sub> could increase the surface-free energy of asphalt, which had greater adhesion energy with the aggregate [21]. Marinho et al. evaluated the effect of nano-TiO<sub>2</sub> as modifiers to improve the rutting resistance and alleviate the fatigue cracking of asphalt mixtures [23]. The results showed that 3% nano-TiO<sub>2</sub> effectively increased the fatigue life and resistance to permanent deformations. Qian et al. reported that the 5% nano-TiO<sub>2</sub> asphalt mixture exhibited an NO<sub>2</sub> degradation productive effect under UV irradiation to reduce environmental pollution [24]. Ye and Chen reported the effect of nano-TiO<sub>2</sub> particles on the temperature properties of AH-70 base asphalt and found that the softening points of the modified asphalt with 0.5% nano-TiO<sub>2</sub> increased by 5°C, and the ductility at 5°C decreased by approximately 22.5 mm compared to those of base asphalt [25]. Sun et al. showed that nano-TiO<sub>2</sub> modified asphalt had more stable ductility and a smaller softening point changing ratio than the base asphalt, and thus, nano-TiO<sub>2</sub> particles actively enhanced the photooxidation resistance of asphalt, and the nano-TiO<sub>2</sub> modified asphalt could resist UV ageing [26]. In a word, adding appropriate amount of nanomaterials can effectively improve the physical properties and rheological properties of base asphalt, but the special environmental characteristics in high-altitude areas need the higher performance of nanomodified asphalt.

The compatibility between base asphalt and copolymer SBS has a strong effect on the low-temperature performance of the modified asphalt [8]. However, nanomaterials can significantly improve the compatibility between polymer and base asphalt. Therefore, many researchers have pay attention to the performance of nanomaterial/polymer modified bitumen. For example, Kang et al. [27], Xiao and Li [28], and Fang et al. [29] found that the nano-ZnO could promote even dispersion of SBS in asphalt, which reduced the free energy of SBS fine particles and improved the adhesion ability of SBS and asphalt interface. Zhang et al. studied the effects of nano-ZnO, nano-TiO<sub>2</sub>, and copolymer SBS on the high- and low-temperature properties for SK-70 base asphalt and the dispersion role of nanomaterials between copolymers and base asphalt. Their results indicated that nanomaterials could effectively improve the dispersion of copolymer SBS and significantly enhanced the high- and low-temperature properties of modified asphalt [30]. Zhang et al. discussed the influence of the multidimensional nanomaterials composed of 1% organic expanded vermiculite (OEVMT) plus 2% nano-TiO<sub>2</sub>, 2% nano-SiO<sub>2</sub>, or plus 2% nano-ZnO on rheological performance of SBS-modified

asphalt (SBSMA) and found that other two multidimensional nanomaterials improved rutting performances and increased thermal cracking resistance of SBSMA except for 1% OEVMT plus 2% nano-SiO<sub>2</sub> [31]. Fang et al. discussed the influence of nanomaterials (nano-TiO<sub>2</sub>, nano-SiO<sub>2</sub>, and nano-ZnO) and isocyanate on performance of base asphalt [12]. Wang et al. showed the influence of the multidimensional nanomaterials composed of 1% organic expanded vermiculite (OEVMT) plus 2% nano-TiO<sub>2</sub>, 2% nano-SiO<sub>2</sub>, or plus 2% nano-ZnO on rheological performance of asphalt and asphalt mixture and found that the multidimensional nanomaterials increased the high-temperature properties and decreased the low-temperature continuous grading [14]. Therefore, the addition of nanomaterials (nano-TiO<sub>2</sub> or nano-ZnO) has improved the physical performance and rheological performance; however, the research on the effect of the interaction between nano-TiO<sub>2</sub> and nano-ZnO on the properties of modified asphalt is not perfect.

In the above studies, many researchers focused on the effect of nanomaterials or copolymer SBS on the properties of asphalt. There has been no perfection of nanomaterial/copolymer SBS in high-altitude areas, especially with respect to the UV antiageing properties of SBS-modified asphalt with the same dimensional different nanomaterials compound modified. Therefore, nano-ZnO, nano-TiO<sub>2</sub>, and copolymer SBS were used to modify AH-90 base asphalt. The optimum content nanomaterial/copolymer SBS for AH-90 base asphalt was selected through physical property tests. Then, the effect of the nanomaterial on the durability properties was studied by beam bending rheometer (BBR) tests and UV ageing test. Furthermore, the morphology, modification mechanism, and UV ageing mechanism of nanomaterial/copolymer SBS were studied by optical microscopy, scanning electron microscopy (SEM), and Fourier transform infrared (FTIR).

## 2. Raw Materials and Experiments

**2.1. Raw Materials.** The base asphalt AH-90 in this paper was provided by Pengsheng Asphalt Co. Ltd. (Henan province, China), and its physical properties are shown in Table 1. The physical properties of nano-ZnO and nano-TiO<sub>2</sub> are shown in Table 2. The properties of copolymer SBS are shown in Table 3.

Methacryloxypropyltrimethoxysilane (C<sub>9</sub>H<sub>20</sub>O<sub>5</sub>Si; KH-560) is a type of surface modification in the field of composite materials [9, 22, 32]. In this study, methacryloxypropyltrimethoxysilane was diluted with distilled water and methanol. The concentration of methacryloxypropyltrimethoxysilane was 20% of the mixing suspensions by weight.

**2.2. Preparation of Modified Asphalt.** Considering the related research results [9, 13, 28, 30, 32, 33], the modified asphalt was prepared as follows. Firstly, the nanomaterials were placed in a vacuum drying chamber at 80°C for 240 minutes, and the base bitumen was heated to 140°C. Secondly, nanomaterial was added in the mixing suspension according the mass fraction and blended at 25°C for 30 minutes; the rotating speed gradually reached 2000 rpm, and the modified

nanomaterials were placed in an air blast drying chamber at 130°C for 120 minutes. Thirdly, in order to give full play to the characteristics of nanomaterial and improve the dispersion effect of SBS in base asphalt [22, 28, 32], appropriate amounts of modified nanomaterials were added into the melt base asphalt and mixed for 120 min with the precision magnetic mixer at 4000 rpm; then, the nanomaterial-modified asphalt was obtained. Fourthly, appropriate amounts of copolymer SBS were added into the nanomaterial-modified asphalt, and the temperature was increased to 180°C for 40 minutes using a high-speed shearing machine with the rotational speed of 4500 rpm. Then, the composite-modified asphalt was put into an oven for 120 minutes to well mix the nanomaterial/copolymer SBS-modified asphalt.

### 2.3. Experimental Design

**2.3.1. Orthogonal Experimental.** The orthogonal experimental design (OED) can strongly decrease the experiment quantity and increase the work efficiency [30, 34]. Hence, the OED method was used to analyse the effect of these modifiers. According to the existing research results [2, 5, 9, 10, 13, 22, 30, 31, 33], the nano-ZnO content in the base asphalt was selected as 3 wt%, 4 wt%, and 5 wt%, and the nano-TiO<sub>2</sub> content in the base asphalt was selected as 0.5 wt%, 1.5 wt%, and 3 wt%; then, the copolymer SBS content in the base asphalt was selected as 2.7 wt%, 3.2 wt%, and 3.7 wt%. This experimental scheme is shown in Table 4.

**2.3.2. UV Aging Test.** To simulate UV irradiation in high-altitude areas, the UV ageing environment oven was designed. The 1000 W high-pressure mercury lamp was a simulated UV light source, and its performance parameters are shown in Table 5. The main spectrum of the high-pressure mercury lamp is 365.0 nm wavelength ultraviolet light, and its wave had the most obvious ageing effect on the asphalt binder [35, 36]. To prevent the asphalt from thermal ageing and maintain it at 35°C in the UV ageing oven, the 200 W axial flow blower was used to supply sufficient cold air, and the 100 W exhaust fan in the top of the oven was used to discharge warm air [37, 38]. The average UV density on the sample surface was approximately 370 W/m<sup>2</sup>.

The UV ageing samples were prepared as follows. Firstly, the thin-film oven test (TFOT) was implemented according to the Chinese Standard Test Methods of Petroleum Asphalt Film Oven Test (JTG E20-2011) [39]. Secondly, the asphalt specimens aged by the TFOT were put into the preheated silica gel abrasive tool with a 140 mm inner diameter and a 1 cm depth to prepare a thin asphalt film with the thickness of approximately 3.2 mm, which was cooled to the sample temperature. Finally, the asphalt specimens were put into the UV ageing oven for 10 days.

### 2.4. Test Method

**2.4.1. Physical Property and BBR Test.** The physical properties of all tested asphalts in this paper, including softening point, penetration (5°C), and ductility (5°C), were tested according to the standard test methods in China test

TABLE 1: Physical properties of base asphalt.

| Property                                | AH-90                           |      |
|---|---------------------------------|------|
| Penetration (25°C, 100 g, 5 s)/(0.1 mm) | 88                              |      |
| Softening point $T_{R\&B}$ (°C)         | 46                              |      |
| Ductility (15°C, 5 cm/min) (cm)         | >100                            |      |
| After RTFOT 163°C, 85 min               | Mass loss (%)                   | 0.40 |
|   | Penetration ratio of 25°C (%)   | 60.0 |
|   | Ductility (15°C, 5 cm/min) (cm) | 12.8 |

TABLE 2: Properties of nano-ZnO and nano-TiO<sub>2</sub>.

| Molecular formula | SSA (m <sup>2</sup> /g) | Crystallite size (nm) | Purity (%) | Color        | Crystal form |
|-------------------|-------------------------|-----------------------|------------|--------------|--------------|
| ZnO               | >35                     | 30                    | 95         | Light yellow | —            |
| TiO <sub>2</sub>  | >30                     | 20                    | 99         | White        | Rutile type  |

TABLE 3: Physical properties of SBS copolymer.

| Structures | S/B (mass ratio) | Tensile strength (MPa) | 300% constant stress (MPa) | Tensile elongation (%) | Tensile permanent deformation (%) |
|------------|------------------|------------------------|----------------------------|------------------------|-----------------------------------|
| Linear     | 30/70            | 15.0                   | 2.0                        | 700                    | 30                                |

TABLE 4: Design of orthogonal experimental.

| Test number | Factors           |                                |              |
|-------------|-------------------|--------------------------------|--------------|
|             | A<br>Nano-ZnO (%) | B<br>Nano-TiO <sub>2</sub> (%) | C<br>SBS (%) |
| 1           | 3.0               | 0.5                            | 2.7          |
| 2           | 3.0               | 1.5                            | 3.2          |
| 3           | 3.0               | 3.0                            | 3.7          |
| 4           | 4.0               | 0.5                            | 3.2          |
| 5           | 4.0               | 1.5                            | 3.7          |
| 6           | 4.0               | 3.0                            | 2.7          |
| 7           | 5.0               | 0.5                            | 3.7          |
| 8           | 5.0               | 1.5                            | 2.7          |
| 9           | 5.0               | 3.0                            | 3.2          |

TABLE 5: Technical parameters of 1000 W high-pressure mercury lamp.

| Types   | Photoelectric parameters |             |             | Geometric parameter |               | Wavelength (nm) |
|---------|--------------------------|-------------|-------------|---------------------|---------------|-----------------|
|         | Power (W)                | Voltage (V) | Current (A) | Length (mm)         | Diameter (mm) |                 |
| GY-1000 | 1000                     | 135         | 8.1         | 225                 | 25            | 365             |

specification JTG E20-2011 [39]. According to AASHTO T313-12 [40], the low-temperature performance of the modified asphalt was evaluated at  $-12^{\circ}\text{C}$ ,  $-18^{\circ}\text{C}$ , and  $-24^{\circ}\text{C}$  in the bending beam rheometer (BBR) test.

In order to further evaluate the UV ageing resistance of modified asphalt, combining the results of softening point test, ductility ( $5^{\circ}\text{C}$ ), and BBR test, the increases in softening point ( $\Delta T$ ), ductility retention rate ( $K_D$ ), and creep stiffness ageing index (SAI) are often used to evaluate the UV ageing degree, which can be calculated using equations (1)–(3):

$$\Delta T = \text{Aged softening point} - \text{Unaged softening point}, \quad (1)$$

$$K_D = \frac{\text{Aged ductility value}}{\text{Unaged ductility value}}, \quad (2)$$

$$\text{SAI} = \frac{S_{\text{aged}} - S_{\text{unaged}}}{S_{\text{unaged}}} \times 100. \quad (3)$$

**2.4.2. Micromorphology Characterization.** The micromorphologies of the AH-90 base asphalt, copolymer SBS-modified asphalt, nanomaterial-modified asphalt, and optimal nano-ZnO/nano-TiO<sub>2</sub>/copolymer SBS-modified asphalt are evaluated by scanning electron microscopy (SEM). Both zinc and titanium percentages in the optimal nano-ZnO/nano-TiO<sub>2</sub>/copolymer SBS-modified asphalt were analysed by SEM and energy dispersive spectrometry (EDS). Its morphologies were observed using an optical microscope before and after the UV ageing. The preparation process of the micromorphology test sample is as follows: each sample to be tested of

fluid asphalt is put into the silica gel abrasive tool with a thickness of about 1 mm. The silica gel abrasive tool was cooled down to room temperature and then 3 samples of  $5 \times 5 \text{ mm}^2$  from different places of the silica gel abrasive tool to ensure repeatability of the result. The above samples are gold coated through the special machine, and then imaging from the section of base and modified asphalt is performed by SEM.

**2.4.3. Microstructure Characterization.** Nano-ZnO and nano-TiO<sub>2</sub> were characterized by FTIR before and after the modification. The modification mechanism of the composite-modified asphalt was also analysed; the scan was from  $400 \text{ cm}^{-1}$  to  $4000 \text{ cm}^{-1}$  at a resolution of  $4 \text{ cm}^{-1}$ . The preparation process of the FTIR test sample is as follows: firstly, a certain amount of dried potassium bromide (KBr) powder was pressed into sheet with good transparency through the table *t* machine. Secondly, the C<sub>2</sub>S solution with 5% asphalt was dropped onto the potassium bromide plate. Finally, the plate is placed into the apparatus for scanning, when the C<sub>2</sub>S solution in the tablet is completely volatilized. Each asphalt is prepared 3 samples, and each sample is scanned 3 times.

Carbonyl group C=O and sulfoxide group S=O were monitored to characterize the UV ageing degree of asphalt [41, 42]. FTIR was further used to monitor these functional groups. The areas of the carbonyl and sulfoxide contents (approximately  $1600 \text{ cm}^{-1}$  and  $1030 \text{ cm}^{-1}$ ) were divided by the entire area between 2000 and  $600 \text{ cm}^{-1}$  to calculate the carbonyl index and sulfoxide index using formulas (4) and (5) [37, 38, 41, 42]:

$$I_{\text{C=O}} = \frac{\text{Area of carbonyl band centered around } 1600 \text{ cm}^{-1}}{\sum \text{Area of spectral bands between } 2000 \text{ and } 600 \text{ cm}^{-1}}, \quad (4)$$

$$I_{\text{S=O}} = \frac{\text{Area of sulphoxide band centered around } 1030 \text{ cm}^{-1}}{\sum \text{Area of spectral bands between } 2000 \text{ and } 600 \text{ cm}^{-1}}. \quad (5)$$

### 3. Results and Discussion

#### 3.1. Proportion of Nano-ZnO/Nano-TiO<sub>2</sub>/Copolymer SBS-Modified Asphalt

**3.1.1. Analysis of Range (ANOR).** The effects of nanoparticles and polymer modifier on physical properties of AH-90 base asphalt are shown in Table 6. Compared with base asphalt, both the softening points and ductilities of nine formulations have also increased markedly, and the penetrations decrease significantly. It indicated that the base asphalt is enhanced in high-temperature performance and low-temperature ductility after adding nanoparticles and polymer modifier. Softening point used to describe the high-temperature performance of asphalt is one of the indexes in most countries. Compared with the base asphalt, the softening point of test number 5 modified asphalt is increased the most obviously, reaching  $76.0^\circ\text{C}$ , which is increasing by

$30^\circ\text{C}$ . Xu et al. indicated that the softening point value of modified asphalt increased about  $56^\circ\text{C}$  when the nano-ZnO dosage was 4.0% in base asphalt [13]. And Qian et al. showed that the rutting factor of SBS-modified asphalt with 1% nano-TiO<sub>2</sub> increased about 2.5 kPa at  $76^\circ\text{C}$  [24]. Zhang Hongliang et al. indicated that the rutting factor of 3.0% nano-ZnO/0.5% nano-TiO<sub>2</sub>/3.7% SBS-modified asphalt at  $88^\circ\text{C}$  is 2.2 kPa which is above the limit (1.0 kPa) provided by AASHTO [30]. Therefore, the suggested asphalt formula meets the requirements of high-temperature stability. Compared with the base asphalt, the ductilities of 9 formulations increase by 16.1 cm at least. Qian et al. [24] and Ma et al. [43] showed that nano-TiO<sub>2</sub> had no significant effect on the low temperature of base asphalt before UV aging. This may be attributed to the addition of nano-ZnO and polymer SBS [13, 24, 30, 43].

In general, a larger  $R_j$  indicates a more significant factor level [34]. As presented in Table 6, the relationship of the effects of the three modifiers on the physical properties is nano-ZnO > copolymer SBS > nano-TiO<sub>2</sub> according to the climate characteristics in high-altitude areas. The blank column  $R_j$  is much smaller than all factors, which implies that the above orthogonal test is reasonable.

**3.1.2. Analysis of Variance (ANOVA).** The ductility is the preferred indicator of the asphalt pavement performance in high-altitude areas in accordance with the Technical Specifications for Highway Asphalt Pavement Construction (JTJ F40-2004) [44]. As presented in Table 7, factor A (nano-ZnO) is highly significant, factor C (copolymer SBS) is significant, and factor B (nano-TiO<sub>2</sub>) has no effect on the test results. Thus, the addition of nano-ZnO in copolymer SBS-modified asphalt has improved the ductility in high-altitude areas. In addition, the effect ranking of the ductility properties is nano-ZnO > copolymers SBS > nano-TiO<sub>2</sub>, and the effect ranking of the softening point properties is nano-ZnO > copolymers SBS > nano-TiO<sub>2</sub>.

The optimal level of selection factors is related to the required indicators. The larger the indicator is, the better it is and the larger the indicators should be, namely, the largest level in each column  $R_{1j}$ ,  $R_{2j}$ , and  $R_{3j}$ ; otherwise, if the smaller the indicator is, the better it is, the lowest level should be selected [45]. In high-altitude areas, asphalt binder is required to have good low-temperature performance and, at the same time, ultraviolet aging resistance. As presented in Tables 7 and 8, 4% nano-ZnO and 3.2% copolymers SBS have significant effects on the low-temperature properties of asphalt. And Zhang et al. [31] and Liang and Lv [46] indicated that the best content of nano-TiO<sub>2</sub> in improving the antiultraviolet aging ability of base asphalt or modified asphalt was 1%–2%. Therefore, the optimal proportions of nano-ZnO, nano-TiO<sub>2</sub>, and copolymer SBS in the base asphalt are determined as 4% nano-ZnO, 3.2% copolymer SBS, and 1.5% nano-TiO<sub>2</sub>.

**3.2. Evaluation on of Nano-ZnO/Nano-TiO<sub>2</sub>/Polymers SBS-Modified Asphalt in Low-Temperature Properties.** In high-altitude areas, the annual temperature is lower, so the asphalt

TABLE 6: Test results and calculation analysis.

| Test number          | Factor   |       |       |       | Test results $y_i$   |  |                      |
|----------------------|----------|-------|-------|-------|----------------------|--|----------------------|
|                      | A        | B     | C     | D     | Softening point (°C) | Ductility (cm)   | Penetration (0.1 mm) |
|                      | 1        | 2     | 3     | 4     |                      |  |                      |
| 1                    | 3.0      | 0.5   | 2.7   |       | 58.2                 | 32.8   | 51.7                 |
| 2                    | 3.0      | 1.5   | 3.2   |       | 65.7                 | 34.9   | 49.8                 |
| 3                    | 3.0      | 3.0   | 3.7   |       | 60.3                 | 33.8   | 51.2                 |
| 4                    | 4.0      | 0.5   | 3.2   |       | 74.8                 | 36.2   | 45.1                 |
| 5                    | 4.0      | 1.5   | 3.7   |       | 76.0                 | 35.7   | 46.2                 |
| 6                    | 4.0      | 3.0   | 2.7   |       | 68.4                 | 34.3   | 47.5                 |
| 7                    | 5.0      | 0.5   | 3.7   |       | 67.6                 | 31.0   | 49.4                 |
| 8                    | 5.0      | 1.5   | 2.7   |       | 64.2                 | 29.5   | 50.1                 |
| 9                    | 5.0      | 3.0   | 3.2   |       | 66.5                 | 30.6   | 49.6                 |
| Softening point (°C) | $K_{1j}$ | 184.2 | 200.6 | 190.8 | 200.7                | $T = \sum_{i=1}^9 y_i = 601.7,$<br>$\bar{y} = T/9 = 66.86$ |                      |
|                      | $K_{2j}$ | 219.2 | 205.9 | 207.0 | 201.7                |  |                      |
|                      | $K_{3j}$ | 198.3 | 195.2 | 203.9 | 199.3                |  |                      |
|                      | $R_j$    | 11.67 | 3.57  | 5.40  | 0.8                  |  |                      |
| Ductility (cm)       | $K_{1j}$ | 101.5 | 100.0 | 96.6  | 99.1                 | $T = \sum_{i=1}^9 y_i = 298.8,$<br>$\bar{y} = T/9 = 33.20$ |                      |
|                      | $K_{2j}$ | 106.2 | 100.1 | 101.7 | 100.2                |  |                      |
|                      | $K_{3j}$ | 91.1  | 98.7  | 100.5 | 99.5                 |  |                      |
|                      | $R_j$    | 5.03  | 0.47  | 1.30  | 0.37                 |  |                      |
| Penetration (mm)     | $K_{1j}$ | 152.7 | 146.2 | 149.3 | 147.5                | $T = \sum_{i=1}^9 y_i = 440.6,$<br>$\bar{y} = T/9 = 48.96$ |                      |
|                      | $K_{2j}$ | 138.8 | 146.1 | 144.5 | 146.7                |  |                      |
|                      | $K_{3j}$ | 149.2 | 148.3 | 146.8 | 146.4                |  |                      |
|                      | $R_j$    | 4.63  | 0.70  | 1.60  | 0.37                 |  |                      |

Note. "D" means blank column.

TABLE 7: Variance analysis of different influencing factors.

|                      | Source                | Square  | df | Mean square | F       | $F_{1-\alpha}(2, 2)$       | Significance |
|----------------------|-----------------------|---------|----|-------------|---------|----------------------------|--------------|
| Softening point (°C) | Nano-ZnO              | 206.740 | 2  | 103.370     | 213.134 | $F_{1-0.05}(2, 2) = 19.00$ | *            |
|                      | Nano-TiO <sub>2</sub> | 19.080  | 2  | 9.540       | 19.670  |                            |              |
|                      | SBS                   | 49.300  | 2  | 24.650      | 50.825  |                            |              |
|                      | Error                 | 0.970   | 2  | 0.485       |         |                            |              |
| Ductility (cm)       | Nano-ZnO              | 39.810  | 2  | 19.905      | 189.571 | $F_{1-0.05}(2, 2) = 19.00$ | *            |
|                      | Nano-TiO <sub>2</sub> | 0.410   | 2  | 0.205       | 1.952   |                            |              |
|                      | SBS                   | 4.740   | 2  | 2.370       | 22.571  |                            |              |
|                      | Error                 | 0.210   | 2  | 0.105       |         |                            |              |
| Penetration (mm)     | Nano-ZnO              | 33.100  | 2  | 16.550      | 236.429 | $F_{1-0.05}(2, 2) = 19.00$ | *            |
|                      | Nano-TiO <sub>2</sub> | 0.920   | 2  | 0.460       | 5.800   |                            |              |
|                      | SBS                   | 3.390   | 2  | 1.695       | 24.214  |                            |              |
|                      | Error                 | 0.140   | 2  | 0.07        |         |                            |              |

TABLE 8: Test results of base asphalt and modified asphalt before and after UV ageing.

| Asphalt type        | Unaged         |                      | Aged           |                      | $K_D$ (%) | $\Delta T$ (°C) |
|---------------------|----------------|----------------------|----------------|----------------------|-----------|-----------------|
|                     | Ductility (cm) | Softening point (°C) | Ductility (cm) | Softening point (°C) |           |                 |
| 4# modified asphalt | 34.2           | 75                   | 30             | 79.1                 | 87.72     | 4.1             |
| 3# modified asphalt | 32.7           | 64.9                 | 25.9           | 71.8                 | 79.20     | 6.9             |
| 2# modified asphalt | 31.3           | 65.5                 | 23.9           | 76.1                 | 76.36     | 10.6            |
| 1# base asphalt     | 7.9            | 49.8                 | 0.3            | 63.9                 | 3.80      | 14.1            |

pavement must have better low-temperature stability than other regions [2]. Therefore, this paper has focused on the low-temperature creep behaviour of base asphalt (1#), 3.2% SBS-modified asphalt (2#), 4% nano-ZnO + 3.2% SBS-modified asphalt (3#), and 4% nano-ZnO + 1.5% nano-TiO<sub>2</sub> + 3.2% SBS-modified asphalt (4#) to evaluate the

cracking resistance using the bending beam rheometer (BBR). The creep stiffness ( $S$ ) and creep rate ( $m$ ) are shown in Figure 1 at three temperatures of  $-12^\circ\text{C}$ ,  $-18^\circ\text{C}$ , and  $-24^\circ\text{C}$ .

The results in Figure 1 reveal that the creep stiffness  $S$  of the modified asphalt decreases, while the creep slope  $m$

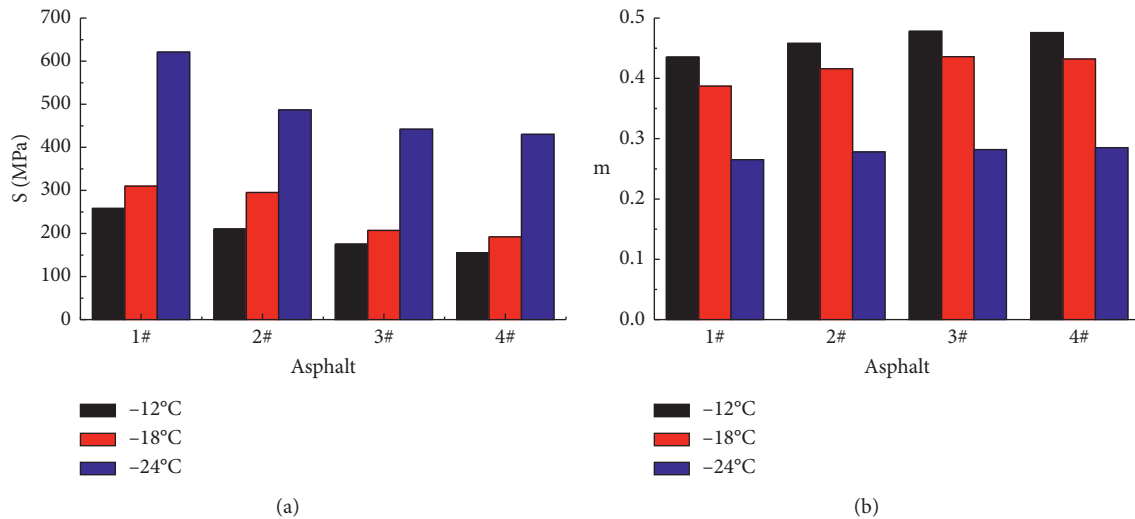


FIGURE 1: Low-temperature properties of base asphalt and modified asphalt. (a) Creep stiffness ( $S$ ). (b) Creep ( $m$ ).

increases with the addition of nanomaterials. Thus, the modified asphalt has better low-temperature performance than the base asphalt. Compared with modified asphalt 2#, modified asphalts 3# and 4# have better resistance to low-temperature cracking, but 4# has no obvious change after the addition of nano-TiO<sub>2</sub>. This result is consistent with the orthogonal test result analysis.

### 3.3. Mechanism of Nano-ZnO/Nano-TiO<sub>2</sub>/Copolymers SBS-Modified Asphalt

**3.3.1. Micromorphology.** To explore the mechanism of the nano-ZnO/nano-TiO<sub>2</sub>/copolymer SBS-modified asphalt, the microstructures of 4% nano-ZnO modified asphalt and surface-modified nano-ZnO modified asphalt were characterized by SEM in addition to the base asphalt (1#), 3.2% SBS-modified asphalt (2#), and 4% nano-ZnO + 1.5% nano-TiO<sub>2</sub> + 3.2% SBS-modified asphalt (4#). These results are shown in Figure 2.

As presented in the nano-ZnO modified asphalt (Figures 2(a) and 2(b)), modified nano-ZnO is more evenly dispersed in the matrix asphalt, the particle size is approximately 32 nm, and the agglomeration phenomenon is obviously weakened. Compared with the morphology of the base asphalt (Figure 2(c)), the morphology of the copolymer SBS-modified asphalt (Figure 2(d)) exhibits floccules of particulate matter with small agglomerate because of the swelling effect of the copolymers SBS after it was absorbed into the oil of the base asphalt, which implies the poor compatibility of copolymer SBS and base asphalt. However, the morphology of copolymer SBS is improved with the addition of nanomaterial (Figures 2(e) and 2(d)), which shows that the copolymer SBS matter decreases in size and is more evenly distributed in the base asphalt. This result is caused by the nanometer size effect of nanoparticles. On one hand, nanoparticles with the active surface area have a strong binding ability to copolymer SBS and base asphalt. On the other hand, the interfacial structure of the

nanomaterials, copolymer SBS, and base asphalt can effectively inhibit the movement of macromolecules to greatly improve the fracture toughness of the base bitumen [28, 30, 33].

**3.3.2. FTIR.** As presented in Figure 3, the absorption peak at 450 cm<sup>-1</sup> and the wide absorption peak at 700 cm<sup>-1</sup> result from the Zn-O stretching vibration in the nano-ZnO lattice and the vibration of Ti-O-Ti in the nano-TiO<sub>2</sub> lattice, respectively. After the surface modification of KH-560, nano-ZnO and nano-TiO<sub>2</sub> have evident absorption peaks at 2941 cm<sup>-1</sup> and 2864 cm<sup>-1</sup>, which belong to the asymmetric stretching vibration and symmetric stretching vibration of -CH<sub>2</sub> with KH-560. Thus, KH-560 has been successfully connected to the surface of nano-ZnO and nano-TiO<sub>2</sub>.

Figure 4 shows the characteristic peak from base asphalt (1#), 3.2% copolymer SBS-modified asphalt (2#), 4% nano-ZnO/3.2% copolymer SBS-modified asphalt (3#), and nano-ZnO/nano-TiO<sub>2</sub>/copolymer SBS-modified asphalt (4#). Compared with the FTIR spectrum of 1#, the 3.2% copolymer SBS-modified asphalt (2#) has no new characteristic peak, except for the characteristic peak of polystyrene at 698 cm<sup>-1</sup> and butadiene at 966 cm<sup>-1</sup>, and it is only a difference in transmission. Therefore, the physical reaction plays the primary role between copolymer SBS and base asphalt. The FTIR of nanomaterials (Figure 3) and modified asphalts 3# and 4# (Figure 4) shows that the absorption peak at 3440 cm<sup>-1</sup> corresponding to the hydroxyl stretching vibration in these nanomaterials disappears, and the transmission of these characteristic peaks produces a larger deviation at approximately 1000 cm<sup>-1</sup> and 400 cm<sup>-1</sup>. Sun et al. indicated that chemical reactions occurred between different substances, and the spectra of the mixtures greatly deviated from those of several components [47]. Therefore, the chemical reactions occurred between both nanomaterials and the base asphalt.

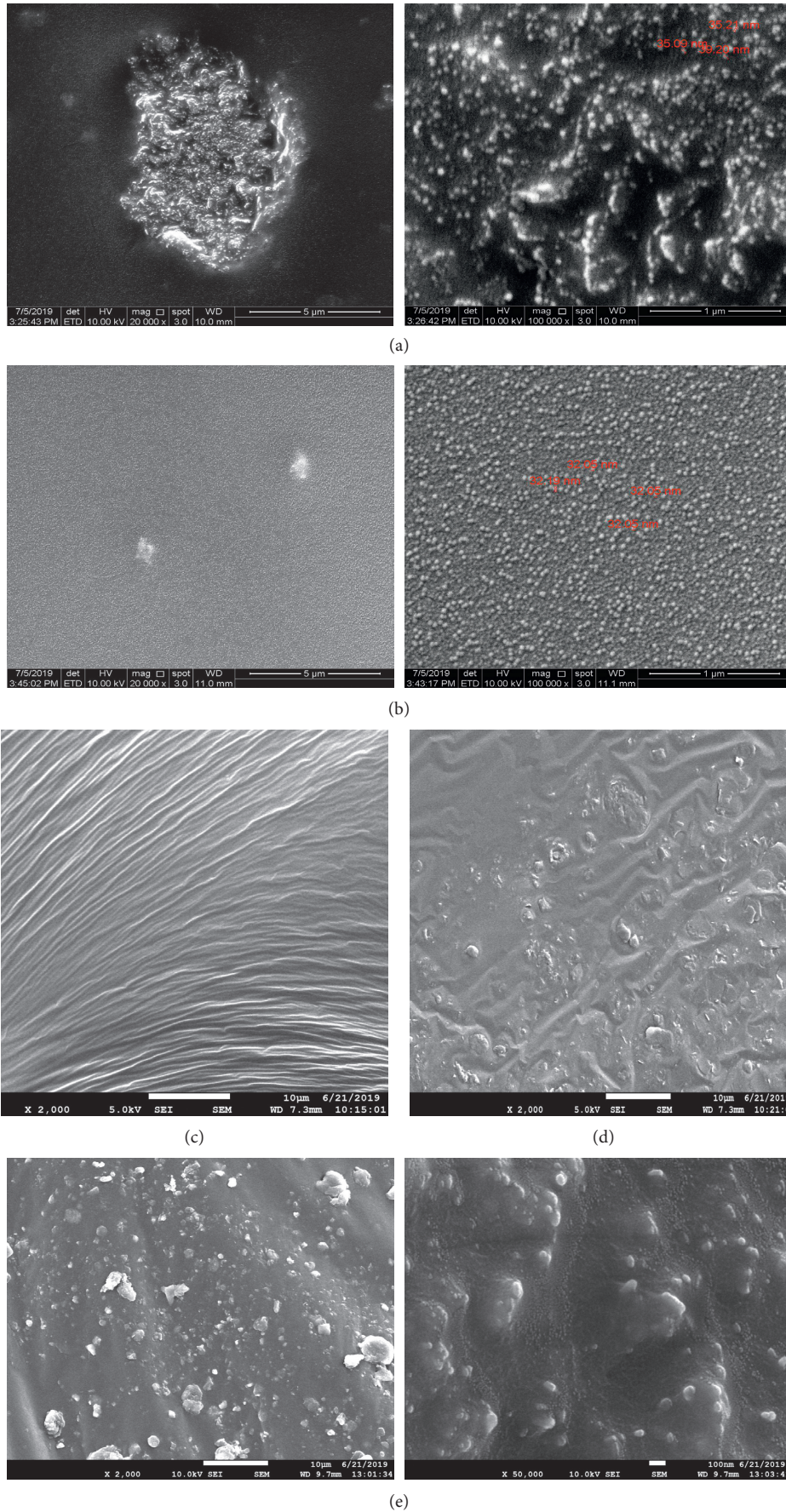


FIGURE 2: The SEM images of base asphalt and modified asphalt. (a) Unmodified nano-ZnO modified asphalt. (b) Surface-modified nano-ZnO modified asphalt. (c) Base asphalt. (d) SBS-modified asphalt. (e) 4# modified asphalt.



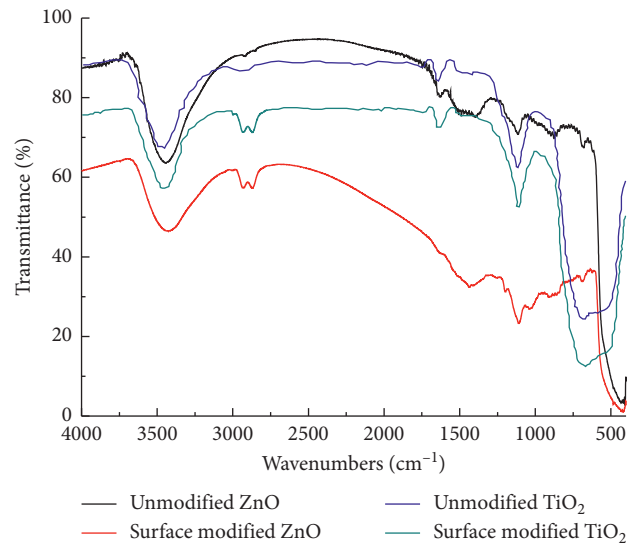


FIGURE 3: FTIR spectra of nanomaterials before and after surface modification by KH-560.

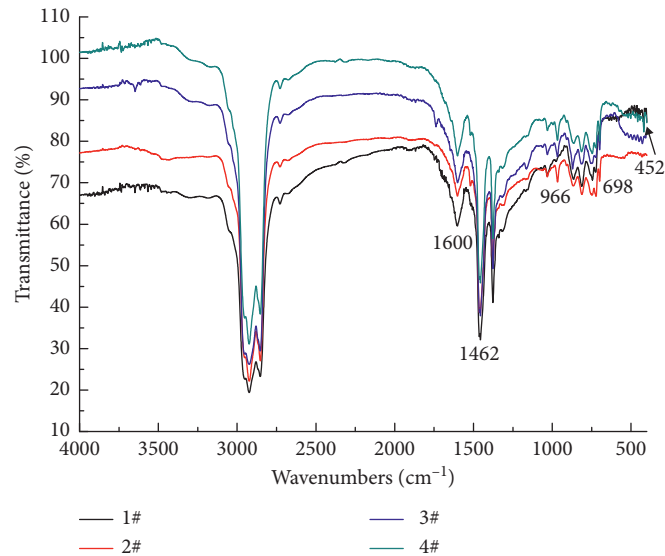


FIGURE 4: FTIR spectra of base asphalt and modified asphalt. 1# (base asphalt), 2# (SBS-modified asphalt), 3# (nano-ZnO/SBS-modified asphalt), and 4# (nano-ZnO/nano-TiO<sub>2</sub>/SBS-modified asphalt).

**3.4. Evaluation of UV Aging Performance of Nano-ZnO/Nano-TiO<sub>2</sub>/Copolymers SBS-Modified Asphalt.** The UV ageing performance of 4% nano-ZnO + 1.5% nano-TiO<sub>2</sub> + 3.2% copolymers SBS-modified asphalt (4#) was investigated in addition to the base asphalt (1#), 3.2% SBS-modified asphalt (2#), and 4% nano-ZnO + 3.2% SBS-modified asphalt (3#).

**3.4.1. Analysis of Physical Performance.** The experimental results of the physical properties (5°C ductility and softening point) of the base asphalt and modified asphalts are shown in Table 8 before and after UV ageing. The modified asphalts have smaller increases in softening point ( $\Delta T$ ) and larger ductility retention rates ( $K_D$ ) than the base asphalt. Modified asphalt 4# had the lowest  $\Delta T$  and highest  $K_D$ . Thus, 4# has the lightest UV ageing degree. Compared to the 2# modified

asphalt,  $K_D$  of 3# and 4# increased from 79.20% to 87.72%;  $\Delta T$  of 3# and 4# decreased from 6.9°C to 4.1°C. The addition of nano-ZnO and nano-TiO<sub>2</sub> to the modified asphalt improves the ability of UV-aging resistance, and nano-TiO<sub>2</sub> has a more significant improvement. All of these results prove that modified asphalt 4# has the best antiaging ability after UV irradiation.

**3.4.2. Cryogenic Performance Analysis.** Low-temperature cracking is the principal reason of asphalt pavement roughness and lower service life in high-altitude areas. The creep stiffness ( $S$ ) and creep rate ( $m$ ) at -18°C are obtained and shown in Figures 5(a) and 6(b) before and after UV ageing. The creep stiffness ( $S$ ) of all asphalts increased after UV radiation, while the creep rate ( $m$ ) reduced. Lower  $S$

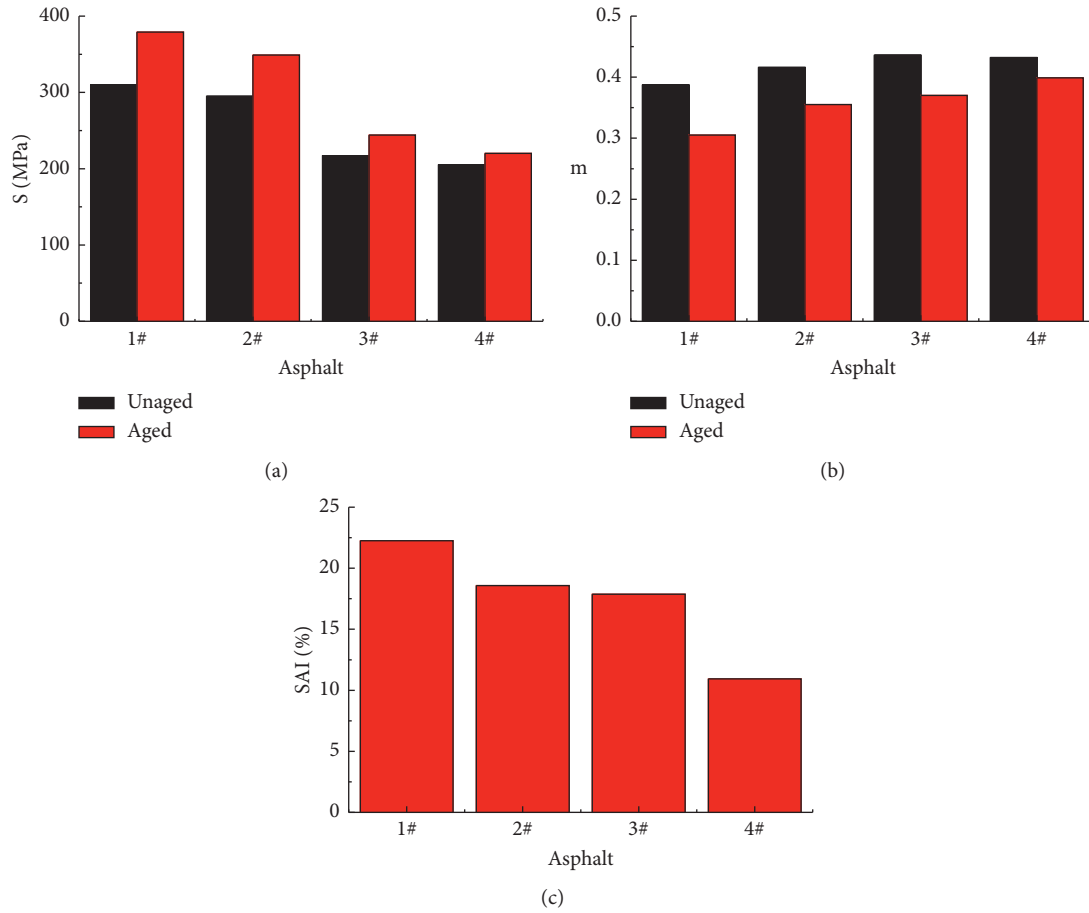


FIGURE 5: These parameters of the UV antiageing properties on base asphalt and modified asphalt. (a) Creep stiffness ( $S$ ). (b) Creep rate ( $m$ ). (c) The creep stiffness ageing index (SAI).

corresponds to higher susceptibility to low-temperature cracking of the asphalt, and higher  $m$  indicates the lower change rate of stiffness with the loading time [3]. Therefore, modified asphalt 4# is less susceptible to low temperature among all asphalts. Figure 5(c) shows the UV ageing indices of the base asphalt and modified asphalt. Compared with the base asphalt, the stiffness ageing index (SAI) of the modified asphalt gradually reduced. Meanwhile, the SAI has no obvious difference between modified asphalts 2# and 3#. These results imply that the 4# modified asphalt has more resistance to low-temperature cracking, which is consistent with  $K_D$ .

### 3.4.3. Morphological/EDS Analysis

(1) *Optical Microscope Image Analysis.* From the optical microscope test, images of base asphalt, pure nano-ZnO, pure nano-TiO<sub>2</sub>, and 4% nano-ZnO + 1.5% nano-TiO<sub>2</sub> + 3.2% copolymer SBS-modified asphalt (4#) are shown in Figures 6 and 7. As shown in Figure 6(a), the morphological character of base asphalt is yellow-orange with a halogen lamp, the pure nano-ZnO is mostly light red (Figure 7(a)), and the pure nano-TiO<sub>2</sub> is dark brown due to the poor light transmission (Figure 7(b)). Thus, the dark substance is nano-TiO<sub>2</sub> in Figure 6(b), and the light red substance is nano-ZnO.

Compared to Figure 6(b), the number of nano-ZnO particles decreased, while nano-TiO<sub>2</sub> had no obvious change after the UV irradiation. Zhang et al. indicated that nano-ZnO had a photolysis reaction under UV irradiation, while nano-TiO<sub>2</sub> did not [48]. Therefore, nano-ZnO in the 4# modified asphalt can cause photolysis.

(2) *SEM/EDS Analysis.* The micromorphology of modified asphalt #4 before and after UV ageing is shown in Figure 8. The number of the large particles decreased after UV ageing on a scale of 200  $\mu\text{m}$  or 100  $\mu\text{m}$ . Considering the particle size, that is, copolymer SBS > nano-ZnO > nano-TiO<sub>2</sub>, the copolymer SBS may degrade. To analyse the content changes of Zn and Ti elements before and after UV ageing, Figures 8(a) and 8(b) were further investigated using the energy dispersive spectrometry (EDS), and the results are shown in Table 9.

As shown in Table 9, the weight percentage of Zn and Ti elements in modified asphalt 4# changed before and after UV ageing. The weight percentage change rate of Zn decreased by 82.70%, and that of Ti decreased by 13.73%. The UV ageing degree of nano-ZnO is more than that of nano-TiO<sub>2</sub>. This result is consistent with the results of Zhang et al. [48]. Nano-ZnO is susceptible to UV photocorrosion, which causes the loss of Zn<sup>2+</sup>. Therefore, the ductility retention rate

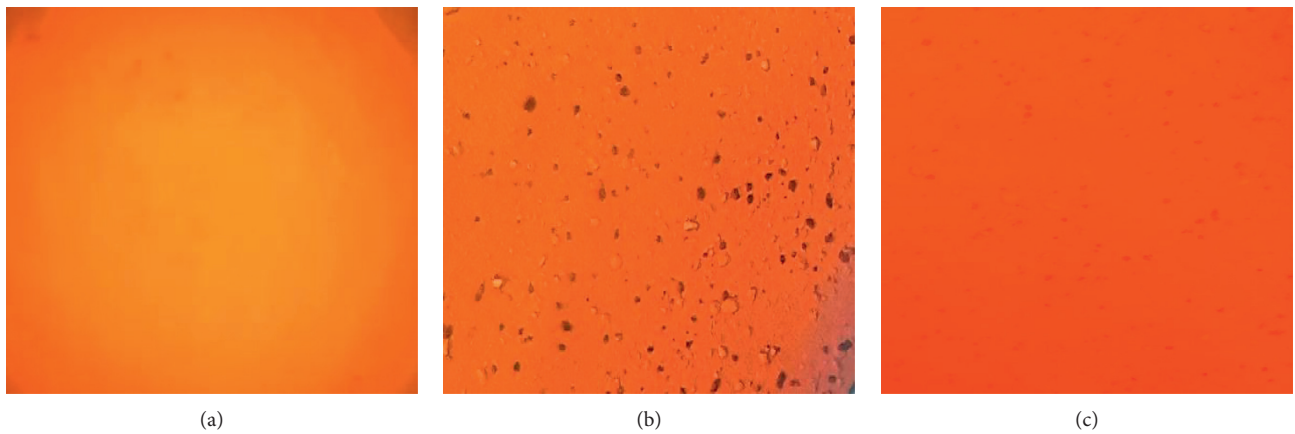


FIGURE 6: The optical microscope image of base asphalt and modified asphalt. (a) Base asphalt. (b) 4# modified asphalt (unaged). (c) 4# modified asphalt (aged).

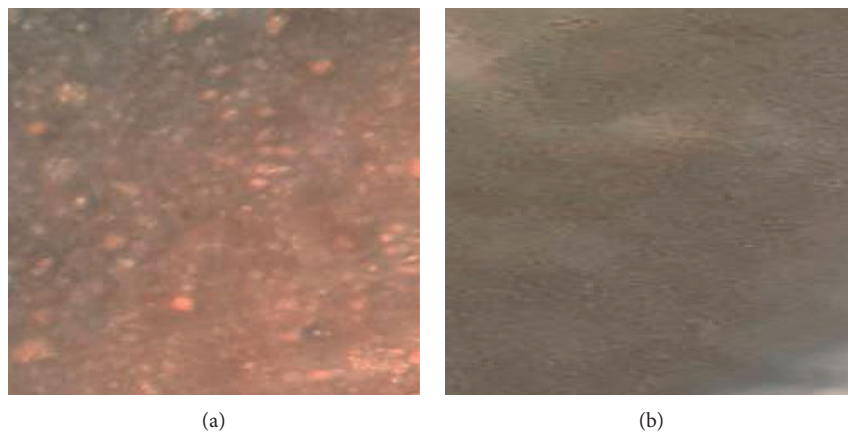


FIGURE 7: The optical microscope image of nanomaterials. (a) Nano-ZnO particle. (b) Nano-TiO<sub>2</sub> particle.

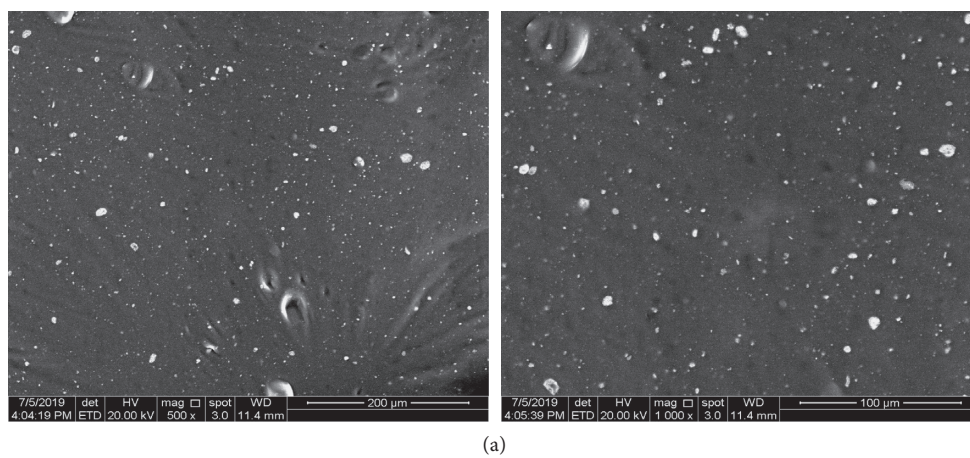


FIGURE 8: Continued.

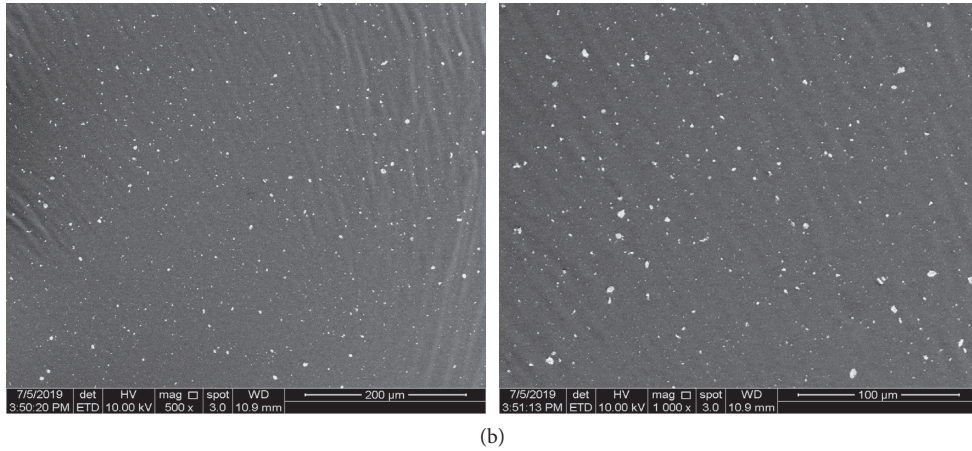


FIGURE 8: The micromorphology of nano-ZnO/nano-TiO<sub>2</sub>/copolymers SBS-modified asphalt. (a) Unaged. (b) Aged.

TABLE 9: EDS test results of nano-ZnO/nano-TiO<sub>2</sub>/copolymers SBS-modified asphalt before and after UV ageing.

| Element | Unaged |        | Aged   |        |
|---------|--------|--------|--------|--------|
|         | Wt (%) | At (%) | Wt (%) | At (%) |
| C       | 88.28  | 95.77  | 84.71  | 91.43  |
| O       | 2.18   | 1.76   | 8.44   | 6.76   |
| S       | 3.68   | 1.48   | 3.16   | 1.27   |
| Ti      | 1.53   | 0.14   | 1.32   | 0.08   |
| Zn      | 4.33   | 0.85   | 2.37   | 0.46   |

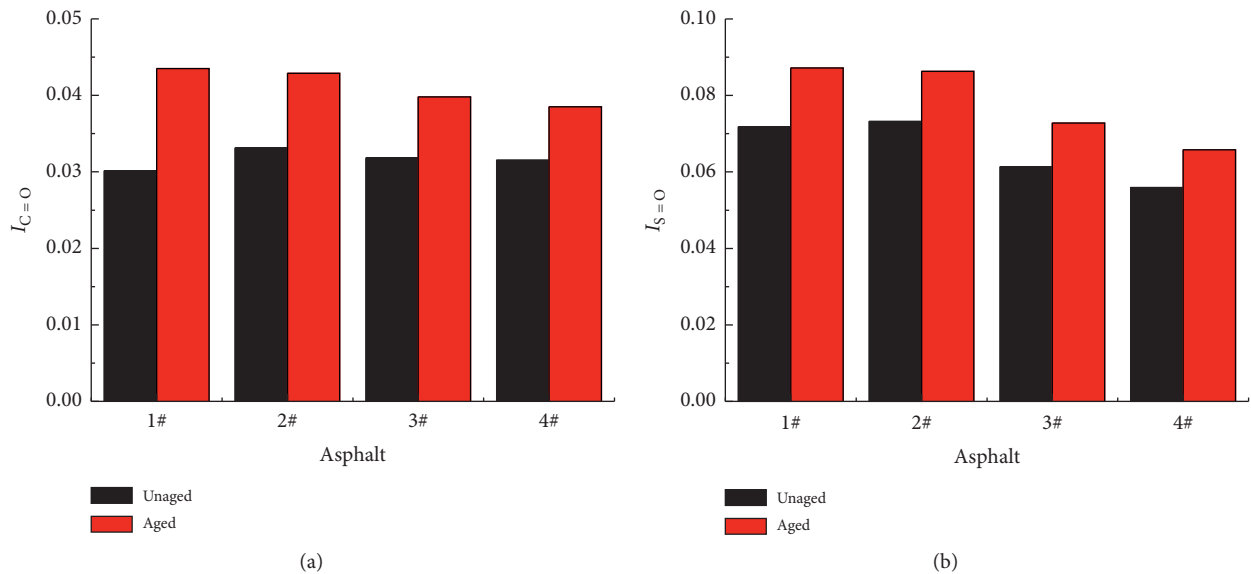


FIGURE 9: The Characteristic functional groups index of asphalt before and after UV ageing. (a) The carbonyl group index ( $I_{C=O}$ ). (b) The sulfoxide group index ( $I_{S=O}$ ).

( $K_D$ ) of the nano-ZnO/copolymer SBS-modified asphalt (3#) increases less obviously than that of copolymer SBS-modified asphalt (2#), while the addition of nano-TiO<sub>2</sub> improves  $K_D$  of modified asphalt 3#, that is, modified asphalt 4#.

3.4.4. FITR. To evaluate the UV ageing degree of the base asphalt and three modified asphalt, the carbonyl group index and sulfoxide group index were calculated according to formulas (4) and (5). Figure 9 shows that both indices of all asphalts are higher than those of unaged asphalt, especially

the carbonyl group index. This conclusion was proven by Hosseinnzhad et al., where the UV ageing affected the carbonyl group index of asphalt more than thermal ageing [49]. The base asphalt has the highest index after UV ageing. A lower index indicates better antiageing property [36, 37]. Therefore, the relationships of the antiageing degree of the base asphalt and modified asphalt are 4# modified asphalt >3# modified asphalt >2# modified asphalt >1# base asphalt. Compared with modified asphalts 2#, the addition of nano-ZnO and nano-TiO<sub>2</sub> in SBS-modified more effectively improves the UV ageing than SBS-modified asphalt. This is mainly because that nanomaterials have the absorption effects on ultraviolet irradiation. Moreover, the addition of nano-TiO<sub>2</sub> in 3# modified bitumen shows the lowest carbonyl group index and sulfoxide group index among the two modified bitumens, which is in accordance with the physical properties test results and cryogenic performance analysis.

#### 4. Conclusions

To improve the UV antiageing and low-temperature properties of AH-90 base asphalt, in this paper, nano-ZnO, nano-TiO<sub>2</sub>, and copolymer SBS were selected as modifiers. The most appropriate amounts of the three modifiers were proposed to modify AH-90 base asphalt. The UV antiageing and low-temperature properties of nano-ZnO/nano-TiO<sub>2</sub>/copolymer SBS-modified asphalt were studied in optimal content. Both SEM/EDS test and FTIR test were used to explain the UV ageing mechanism of nano-ZnO/nano-TiO<sub>2</sub>/copolymer SBS-modified asphalt. The following conclusions are drawn:

- (i) The surface functionalization of nano-ZnO and nano-TiO<sub>2</sub> using KH-560 can turn nano-ZnO and nano-TiO<sub>2</sub> to a highly effective additive to enhance the UV ageing resistance and low-temperature performance of copolymer SBS-modified asphalt.
- (ii) The orthogonal test and BBR test show that the copolymer SBS significantly affects the low-temperature performance of the nano-ZnO/nano-TiO<sub>2</sub>/copolymer SBS-modified asphalt, and nano-ZnO has a highly significant effect on its low-temperature performance. The most appropriate amount of three modifiers to add is 4% nano-ZnO + 1.5% nano-TiO<sub>2</sub> + 3.2% copolymer SBS.
- (iii) The SEM test shows that the addition of nanomaterials can improve the dispersion of copolymer SBS in asphalt due to the encapsulation and dispersion of nanomaterials. The EDS test result shows that the nano-ZnO particles are prone to photocorrosion and reduce the activity under ultraviolet irradiation, so nano-ZnO/copolymer SBS-modified asphalt has less obvious antiaging performance than the copolymer SBS-modified asphalt. Furthermore, adding nano-TiO<sub>2</sub> in nano-ZnO/copolymer SBS-modified asphalt will improve its UV antiageing performance.
- (iv) The FTIR test shows that the blending mechanism of nano-ZnO/nano-TiO<sub>2</sub>/copolymer SBS-modified asphalt is that the physical reaction is more dominant for both SBS copolymers and base asphalt, and the chemical reactions mainly occur between nanomaterials and base asphalt in the modification process. The carbonyl group index and sulfoxide group index results indicate that ultraviolet irradiation has the most significant effect on the carbonyl index of the nano-ZnO/nano-TiO<sub>2</sub>/copolymer SBS-modified asphalt, which has the best UV antiageing performance.

#### Data Availability

The data used to support the findings of this study are available from the corresponding author upon request.

#### Conflicts of Interest

The authors declare they have no conflicts of interest.

#### Acknowledgments

The authors are grateful for financial support from the Key Project of Colleges and Universities of Henan Province (19A560024), National Students' Project for Innovation and Entrepreneurship Training Program (201810485005), Fund of Leading Talent in Science and Technology Innovation (194200510015), and Science and Technology Department of Henan Province (182300410198, 192102310012, and 202102310589).

#### References

- [1] H. Liu, B. Hu, L. Zhang et al., "Ultraviolet radiation over China: spatial distribution and trends," *Renewable and Sustainable Energy Reviews*, vol. 76, pp. 1371–1383, 2017.
- [2] D. Zheng, Z.-d. Qian, P. Li, and L.-b. Wang, "Performance evaluation of high-elasticity asphalt mixture containing inorganic nano-titanium dioxide for applications in high altitude regions," *Construction and Building Materials*, vol. 199, pp. 594–600, 2019.
- [3] F. Durrieu, F. Farcas, and V. Mouillet, "The influence of UV aging of a Styrene/Butadiene/Styrene modified bitumen: comparison between laboratory and on site aging," *Fuel*, vol. 86, no. 10-11, pp. 1446–1451, 2007.
- [4] A. Diab, M. Enieb, and D. Singh, "Influence of aging on properties of polymer-modified asphalt," *Construction and Building Materials*, vol. 196, pp. 54–65, 2019.
- [5] D. M. Zhang, *Study on the preparation and properties of multi-scale nanomaterials/SBS modified asphalts*, Hunan University, Changsha, China, Ph.D. dissertation, 2018.
- [6] H. R. Fischer and B. Dillingh, "Response of the microstructure of bitumen upon stress-damage initiation and recovery," *Road Materials and Pavement Design*, vol. 16, no. 1, pp. 31–45, 2015.
- [7] G. Polacco, S. Filippi, F. Merusi, and G. Stastna, "A review of the fundamentals of polymer-modified asphalts: asphalt/polymer interactions and principles of compatibility," *Advances in Colloid and Interface Science*, vol. 224, pp. 72–112, 2015.

- [8] A. Behnood and M. Modiri Gharehveran, "Morphology, rheology, and physical properties of polymer-modified asphalt binders," *European Polymer Journal*, vol. 112, pp. 766–791, 2019.
- [9] R. Li, J. Pei, and C. Sun, "Effect of nano-ZnO with modified surface on properties of bitumen," *Construction and Building Materials*, vol. 98, pp. 656–661, 2015.
- [10] Q. P. Zhu, "Preparation and properties analysis of asphalt modified by nano-ZnO," *Applied Chemical Industry*, vol. 48, no. 5, pp. 1031–1034, 2019.
- [11] H. Y. Liu, H. L. Zhang, P. W. Hao, and C. Z. Zhu, "The effect of surface modifiers on ultraviolet aging properties of nano-zinc oxide modified bitumen," *Petroleum Science and Technology*, vol. 33, no. 1, pp. 72–78, 2015.
- [12] C. Fang, X. Yu, R. Yu, P. Liu, and X. Qiao, "Preparation and properties of isocyanate and nano particles composite modified asphalt," *Construction and Building Materials*, vol. 119, pp. 113–118, 2016.
- [13] X. Xu, H. Guo, X. Wang, M. Zhang, Z. Wang, and B. Yang, "Physical properties and anti-aging characteristics of asphalt modified with nano-zinc oxide powder," *Construction and Building Materials*, vol. 224, pp. 732–742, 2019.
- [14] J. Z. Wang, H. L. Zhang, and C. Z. Zhu, "Effect of multi-scale nanocomposites on performance of asphalt binder and mixture," *Construction and Building Materials*, vol. 243, Article ID 118307, 2020.
- [15] R. Kleizienė, M. Paliukaitė, and A. Vaitkus, "Effect of nano-SiO<sub>2</sub>, TiO<sub>2</sub> and ZnO modification to rheological properties of neat and polymer modified bitumen," *ISAP APE 2019*, Springer, pp. 325–336, Springer, Cham, Switzerland, LNCE 48, 2020.
- [16] M. Saltan, S. Terzi, and S. Karahancer, "Mechanical behavior of bitumen and hot-mix asphalt modified with zinc oxide nanoparticle," *Journal of Materials in Civil Engineering*, vol. 31, no. 3, Article ID 04018399, 2019.
- [17] H. Nazari, K. Naderi, and F. Moghadas Nejad, "Improving aging resistance and fatigue performance of asphalt binders using inorganic nanoparticles," *Construction and Building Materials*, vol. 170, pp. 591–602, 2018.
- [18] H. L. Zhang and D. M. Zhang, "Effect of different inorganic nanoparticles on physical and ultraviolet aging properties of bitumen," *Journal of Materials in Civil Engineering*, vol. 27, no. 12, Article ID 04015049, 2015.
- [19] G. H. Hamedi, F. M. Nejad, and K. Oveisi, "Estimating the moisture damage of asphalt mixture modified with nano zinc oxide," *Materials and Structures*, vol. 49, no. 4, pp. 1165–1174, 2016.
- [20] C. Zhu, H. Zhang, G. Xu, and C. Shi, "Aging rheological characteristics of SBR modified asphalt with multi-dimensional nanomaterials," *Construction and Building Materials*, vol. 151, pp. 388–393, 2017.
- [21] A. R. Azarhoosh, F. M. Nejad, and A. Khodaii, "Using the surface free energy method to evaluate the effects of nanomaterial on the fatigue life of hot mix asphalt," *Journal of Materials in Civil Engineering*, vol. 28, no. 10, pp. 981–989, 2015.
- [22] H. L. Zhang, *Preparation and properties of bitumen/inorganic nanocomposites*, Wuhan University of Technology, Wuhan, China, Ph.D. dissertation, 2012.
- [23] P. Marinho, A. Rodrigues, L. Lucena, and V. Neto, "Rheological evaluation of asphalt binder 50/70 incorporated with titanium dioxide nanoparticles," *Journal of Materials in Civil Engineering*, vol. 31, no. 10, Article ID 04019235, 2019.
- [24] G. Qian, H. Yu, X. Gong, and L. Zhao, "Impact of Nano-TiO<sub>2</sub> on the NO<sub>2</sub> degradation and rheological performance of asphalt pavement," *Construction and Building Materials*, vol. 218, pp. 53–63, 2019.
- [25] C. Ye and H. X. Chen, "Study on road performance of nano-SiO<sub>2</sub> and nano-TiO<sub>2</sub> modified asphalt," *New Building Materials*, vol. 6, pp. 82–87, 2009.
- [26] S. S. Sun, Y. M. Wang, and A. Q. Zhang, "Study on anti-ultraviolet radiation aging property of TiO<sub>2</sub>," *Advanced Materials Research*, vol. 306-307, pp. 951–955, 2011.
- [27] A. H. Kang, P. Xiao, and X. Zhou, "Study on hot storage stability of nanometer ZnO/SBS modified asphalt," *Journal of Jiangsu University*, vol. 31, no. 4, pp. 82–87, 2010.
- [28] P. Xiao and X.-F. Li, "Research on the performance and mechanism of nanometer ZnO/SBS modified asphalt," *Journal of Highway and Transportation Research and Development*, vol. 24, no. 6, pp. 12–16, 2007.
- [29] C. Q. Fang, R. E. Yu, S. L. Liu, and Y. Li, "Nanomaterials applied in asphalt modification: a review," *Journal of Materials Science & Technology*, vol. 29, no. 7, pp. 589–564, 2013.
- [30] H. L. Zhang, M. M. Su, S. F. Zhao, Y. P. Zhang, and Z. P. Zhang, "High and low temperature properties of nanoparticles/polymer modified asphalt," *Construction and Building Materials*, vol. 114, pp. 323–332, 2016.
- [31] D. M. Zhang, Z. H. Chen, H. L. Zhang, and C. W. Wei, "Rheological and anti-aging performance of SBS modified asphalt binders with different multi-dimensional nanomaterials," *Construction and Building Materials*, vol. 188, pp. 409–416, 2018.
- [32] L. Sun, X. T. Xin, and J. L. Ren, "Inorganic nanoparticle-modified asphalt with enhanced performance at high temperature," *Journal of Materials in Civil Engineering*, vol. 29, no. 3, Article ID 04016227, 2017.
- [33] R. Y. Li, P. Xiao, S. Amirkhanian, Z. P. You, and J. Huang, "Developments of nano materials and technologies on asphalt materials-A review," *Construction and Building Materials*, vol. 143, pp. 633–648, 2017.
- [34] L. S. Su, J. B. Zhang, C. J. Wang et al., "Identifying main factors of capacity fading in lithium ion cells using orthogonal design of experiment," *Applied Energy*, vol. 163, pp. 201–210, 2016.
- [35] Y. Y. Li, S. P. Wu, Q. T. Liu et al., "Aging effects of ultraviolet lights with same dominant wavelength and different wavelength ranges on a hydrocarbon-based polymer (asphalt)," *Polymer Testing*, vol. 75, pp. 64–75, 2019.
- [36] J. X. Hu, S. P. Wu, Q. T. Liu et al., "Effect of ultraviolet radiation in different wavebands on bitumen," *Construction and Building Materials*, vol. 159, pp. 479–485, 2018.
- [37] W. B. Zeng, S. P. Wu, J. Wen, and Z. W. Chen, "The temperature effects in aging index of asphalt during UV aging process," *Construction and Building Materials*, vol. 93, pp. 1125–1131, 2015.
- [38] X. B. Xie, S. J. Tong, Y. B. Ding, H. N. Liu, and L. Y. Liang, "Effect of the amount of mineral powder on the ultraviolet aging properties of asphalt," *Advance in Materials Science and Engineering*, vol. 2016, Article ID 5207391, 9 pages, 2016.
- [39] China Communications Press, *Standard Test Methods of Bitumen and Bituminous Mixtures for Highway Engineering*, China Communications Press, Beijing, China, 2011.
- [40] AASHTO T313-12, *Determining the Flexural Creep Stiffness of Asphalt Binder Using the Bending Beam Rheometer (BBR)*, American Association of State Highway and Transportation Officials, Washington, DC, USA, 2012.
- [41] J. Lamontagne, P. Dumas, V. Mouillet, and J. Kister, "Comparison by fourier transform infrared (FTIR)

- spectroscopy of different ageing techniques: application to road bitumens,” *Fuel*, vol. 80, no. 4, pp. 483–488, 2001.
- [42] M. R. Nivitha, E. Prasad, and J. M. Krishnan, “Ageing in modified asphalt using FTIR spectroscopy,” *International Journal of Pavement Engineering*, vol. 17, no. 7, pp. 1–13, 2015.
- [43] B. Ma, J. G. Rong, S. H. Yan et al., “Effect of Nanometer TiO<sub>2</sub> on asphalt ultraviolet aging resistance,” *Highway*, vol. 12, pp. 189–192, 2008.
- [44] China Communications Press, *Technical Specifications for Construction of Highway Asphalt Pavement*, China Communications Press, Beijing, China, 2004.
- [45] C. Q. Zhuang and C. X. He, *Applied Mathematical Statistics*, South China University Technology, Guangzhou, China, 2007.
- [46] H. Liang and B. Lv, “Effect of nanometer TiO<sub>2</sub> in anti-ultraviolet aging in asphalt,” *Journal of Chongqing Jiaotong Uninersicty (Natural Science)*, vol. 32, no. 2, pp. 203–206, 2013.
- [47] L. Sun, X. Xin, H. Y. Wang, and W. J. Gu, “Microscopic mechanism of modified asphalt by multi-dimensional and multi-scale nanomaterial,” *Journal of the Chinse Ceramic Society*, vol. 40, no. 10, pp. 1437–1447, 2012.
- [48] M. Zhang, Q. L. Zhao, P. K. He, J. J. Yang, and Z. S. Jin, “Photocatalytic oxidation of CO on TiO<sub>2</sub> and ZnO,” *Chemical Research*, vol. 16, no. 4, pp. 66–69, 2005.
- [49] S. Hosseinnzhad, M. Zadshir, X. K. Yu, H. M. Yu, B. Sharma, and E. Fini, “Differential effects of ultraviolet radiation and oxidative aging on bio-modified binders,” *Fuel*, vol. 251, pp. 45–56, 2019.